

What Will Argus See?

Steven W. Ellingson*

March 1, 2003

Contents

1	Introduction	2
2	Theory	2
2.1	Detection Sensitivity	2
2.2	Imaging and Localization	4
3	Application to Argus	4
3.1	Single-Element (N=1) Argus	6
3.2	N=8 Argus	6
3.3	N=16 Argus	7
3.4	$N = 64$ Argus	10
A	Source List	13

*The Ohio State University ElectroScience Laboratory, 1320 Kinnear Road, Columbus OH 43212. E-mail: ellingson@ieee.org

1 Introduction

“Argus” is a concept for a radio telescope that has an instantaneous field of view covering most of the visible sky [1]. The primary motivation for this concept is to facilitate a microwave transient observing program, targeting astrophysical pulses as well as ultra-narrowband tones incident from anywhere in the sky [2]. A prototype development project is underway at the Ohio State University ElectroScience Laboratory (ESL), with the interim goal of implementing a 64-element Argus system. Along the way, there will probably also be functioning 8-, 16-, and 32-element systems. A design exists, and most aspects of the hardware performance have been validated experimentally, either in field conditions or in the lab, for a single element. In this report, we predict the performance of the upcoming multi-element systems. This is useful so that one knows what level of performance to expect, and suitable tests can be designed.

2 Theory

For Argus, there are two modes of operation: detection and localization. The requirements for these two modes are different, and it is best to consider them separately. (*Note:* Localization and imaging are essentially the same problem.)

2.1 Detection Sensitivity

For the purposes of this study, the radio sky can be modeled as the sum of two components. The first component, normally not of interest from an Argus perspective, is the brightness temperature of the background sky, $T_{sky}(\theta, \phi)$ (units of K). (*Note:* In the coordinate system used in this report, the zenith is $\theta = 0$.) The second component is a population of M discrete sources, which are modeled as a flux distribution $S(\theta, \phi)$ (units of Jy, where $1 \text{ Jy} = 10^{-26} \text{ W m}^{-2} \text{ Hz}^{-1}$) as follows:

$$S(\theta, \phi) = \sum_{m=1}^M S_m \delta(\theta - \theta_m) \delta(\phi - \phi_m), \quad (1)$$

where $\delta(0) = 1$, and is zero for all other values. It is assumed that all sources are point sources, which is a reasonable approximation for a small Argus system with resolution on the order of 1° or larger.

Suppose we have a perfectly calibrated, alias-free array, such that we are able to point a well-formed beam in the direction of source m . The power measured at the terminals of antenna n due to source m only is

$$P_{n,m} = \frac{1}{2} S_m A(\theta_m, \phi_m) B_m \quad (2)$$

where $A(\theta, \phi)$ is the effective aperture of a single element of the array, and B_m is the bandwidth of the source or of the antenna, whichever is greater. The factor of $\frac{1}{2}$ is due to the fact that we only measure one polarization, whereas the incident power is normally divided across both polarizations. Since a beamformer results in coherent addition of voltages, the power at the output of the beamformer due to source m is

$$P_m = \left[\sum_{n=1}^N P_{n,m}^{1/2} \right]^2 = \frac{1}{2} S_m A(\theta_m, \phi_m) B_m N^2 \quad (3)$$

The beamformer output also includes noise from the receivers, from other directions in the sky, and from the warm ground. The receiver noise power for a single element, referenced to the terminals of the antenna, is

$$Z_{n,r} = kT_r B \quad (4)$$

where k is $1.38 \times 10^{-23} \text{ J/K}$, $T_r \sim 170\text{K}$ for the current generation of Argus receivers¹, and B is the processed bandwidth of the receiver. Assuming that T_r is about the same for all receivers, and that

¹A conservative value based on measurements; see [8] and [9]

the receiver noise is uncorrelated between receivers, the total receiver noise power at the output of the beamformer is

$$Z_r = \sum_{n=1}^N Z_{n,r} = kT_rBN \quad (5)$$

The noise contribution Z_g associated with the ground can be treated in a similar manner, since we expect that this contribution will also be mostly uncorrelated between elements. The per-element contribution – call this T_g – depends on the pattern of the antenna and the composition of the surrounding terrain.

Accurate estimation of the contribution from sky noise – call this Z_a – requires detailed knowledge of $T_{sky}(\theta, \phi)$, the element pattern, and the array geometry. In general,

$$Z_a = kT_aB \quad (6)$$

where T_a is the equivalent antenna temperature at the output of the beamformer due to these contributions.

T_g and T_a are difficult to measure or estimate independently. However, it is possible to develop suitable estimates for some limiting conditions. Here are some considerations:

- For the current design at 1420 MHz, we have experimentally determined the antenna temperature T_A for a single element ($N = 1$) to be on the order of 100K.² In this case, T_A is the sum of T_g , T_a , and the loss associated with the antenna itself. Therefore T_g is upper-bounded (very approximately) at ~ 100 K.
- A very large array forms a single very narrow beam with very low sidelobes far from the main lobe. In this case, $T_a \sim T_{sky}(\theta_m, \phi_m)$. $T_{sky}(\theta_m, \phi_m)$ varies a lot depending on where in the Galaxy (θ_m, ϕ_m) points. When pointing toward the Galactic Center, T_{sky} is dominated by Galactic noise and can be up to ~ 100 K [5](Fig. 7-1, p. 7-1; Fig. 8-60, p. 8-91). Looking away from the Galactic Center (especially out of the plane of the Galaxy), Galactic noise is negligible and T_{sky} instead is the sum of the cosmic microwave background (CMB) at ~ 3 K plus a few K associated with atmospheric losses, for perhaps ~ 6 K total. From Columbus, OH ($\sim 40^\circ$ N latitude), the Galactic center never gets very high in the sky.

Naturally occurring transients have wide bandwidth, filling the bandwidth of the receiver such that $B_m = B$. For SETI, we assume that B is set equal to B_m , where B_m is the dispersion limit of ~ 0.1 Hz. Thus, in either case, we have $B \approx B_m$. Thus, the signal-to-noise ratio (SNR) for source m is

$$\text{SNR} = \frac{P_m}{Z_r + Z_g + Z_a} = \frac{S_m A(\theta_m, \phi_m) N}{2k(T_r + T_g + T_a/N)} \quad (7)$$

If we require $\text{SNR} = 1$ for a detection, then the sensitivity of the system is given by

$$\Delta S = \frac{2k(T_r + T_g + T_a/N)}{A(\theta_m, \phi_m) N} \quad (8)$$

If we can't improve the SNR, then the only way to improve sensitivity is to increase the implied value of $B\tau$ from 1 to some larger value, normally by increasing the integration time τ . In general,

$$\Delta S = \frac{2k(T_r + T_g + T_a/N)}{A(\theta_m, \phi_m) N\sqrt{B\tau}} \quad (9)$$

An important caveat: It should be noted that the above equation is specific to the $M = 1$ case; i.e., we are assuming that the sky is dominated by one discrete source, and that the system is pointing at it. If this is not the case, the “noise equivalent” contribution of the other source(s) must be taken into account. This is most easily considered on a case-by-case basis for various Argus sizes considered in Section 3.

²We estimated ~ 120 K in [8] and ~ 75 K in [9].

2.2 Imaging and Localization

As in detection, imaging and localization are limited by the contribution of the sky background noise filling the beam, and the contributions of other sources coming in through the sidelobes.

Impact of Sky Noise: This is $\sim 6\text{K}$ over most of the sky, occasionally peaking up to $\sim 100\text{K}$ as noted above. The equivalent flux³ can be obtained by equating the power due to the sky noise temperature, $kT_a(\theta, \phi)B$ (assuming the beam is filled at this temperature) to the expected power due to a flux S_a , $\frac{1}{2}S_aA(\theta, \phi)B$. This yields

$$S_a = \frac{2kT_a(\theta, \phi)}{A(\theta, \phi)} \quad (10)$$

(Note the similarity to Equation 8.) To apply Equation 10 to Argus, a reasonable estimate of $A(\theta, \phi)$ is required. Note that the zenith directivity $G(0, 0)$ of the spiral antenna units is approximately 2; thus

$$A(0, 0) = \epsilon \frac{\lambda^2}{4\pi} G(0, 0) \approx 60 \text{ cm}^2, \quad (11)$$

using an experimentally-determined efficiency of $\epsilon = 0.86$ (associated with the match between the antenna and the LNA) at 1420 MHz. Away from the zenith, the pattern rolls off approximately as $\cos \theta$, so we can estimate:

$$A(\theta, \phi) \approx (60 \text{ cm}^2) \cos \theta \quad (\theta < \frac{\pi}{2}). \quad (12)$$

Using these results, the equivalent flux associated with the sky background is plotted in Figure 1. To interpret this result, consider the following example. Assume a sky which is uniformly 6K except for a single point source at the zenith. The equivalent flux due to the sky background is $\sim 50 \text{ kJy}$ for an $N = 64$ element Argus. In this case, the point source must be at least 50 kJy to be imaged (or otherwise localized) with $\text{SNR}=1$, assuming $B\tau = 1$. To improve the sensitivity by a factor of 10 in the image, $B\tau$ must be increased by a factor of $10^2 = 100$. Thus, it is easy to see that the background sky temperature can be a serious impediment to imaging for small- N (small A) arrays.

Impact of strong sources in sidelobes: Again, this is easiest to see by example. Consider a sky which consists of two widely-separated point sources of equal flux, each of which is orders of magnitude stronger than the effective flux associated with the sky background (so that sky noise is not a limitation). When a beam is pointed at one source, the image dynamic range will be equal to the sidelobe level at the point in which the second source enters the pattern. For a modestly-sized (e.g, $N < 100$) Argus, the far sidelobes might only be 5–10 dB down (as will be demonstrated later); so, in the preceding example, the image dynamic range would be only 5–10 dB. If the source in the sidelobes was any stronger, imaging (or localizing) the desired source would be hopeless – unlike the sky noise problem, increasing $B\tau$ will not help here.⁴

3 Application to Argus

To apply Equation 9 to Argus, it remains to determine reasonable values for $B\tau$. For tone searches (SETI), sensitivity is optimized for $B \sim 0.1 \text{ Hz}$. Since the tone may in fact be a pulse, it is also desirable to match τ to the length of the pulse. Since the pulse length is unknown *a priori*, short pulses cannot be ruled out. However, the shortest possible pulse is given by $B\tau = 1$. For astrophysical pulses, sensitivity is optimized by maximizing B . A single Argus Narrowband Processor (ANP) can support $B = 34 \text{ kHz}$ for astrophysical pulse searches, for which the shortest pulse that can be detected at full sensitivity is $\sim 30 \mu\text{s}$. Thus, the worst case scenario for either tones or pulses is $B\tau = 1$ but can be made to be $\gg 1$ by giving up sensitivity to short-duration events.

³The purpose in defining an “equivalent flux” here is simply to obtain expressions in terms of power, which can then be used in SNR calculations. No physical flux is implied.

⁴Image processing methods such as CLEAN can help, but only if there are small number of discrete “noise” sources and a germane beam pattern. These assumptions are generally not valid for Argus.

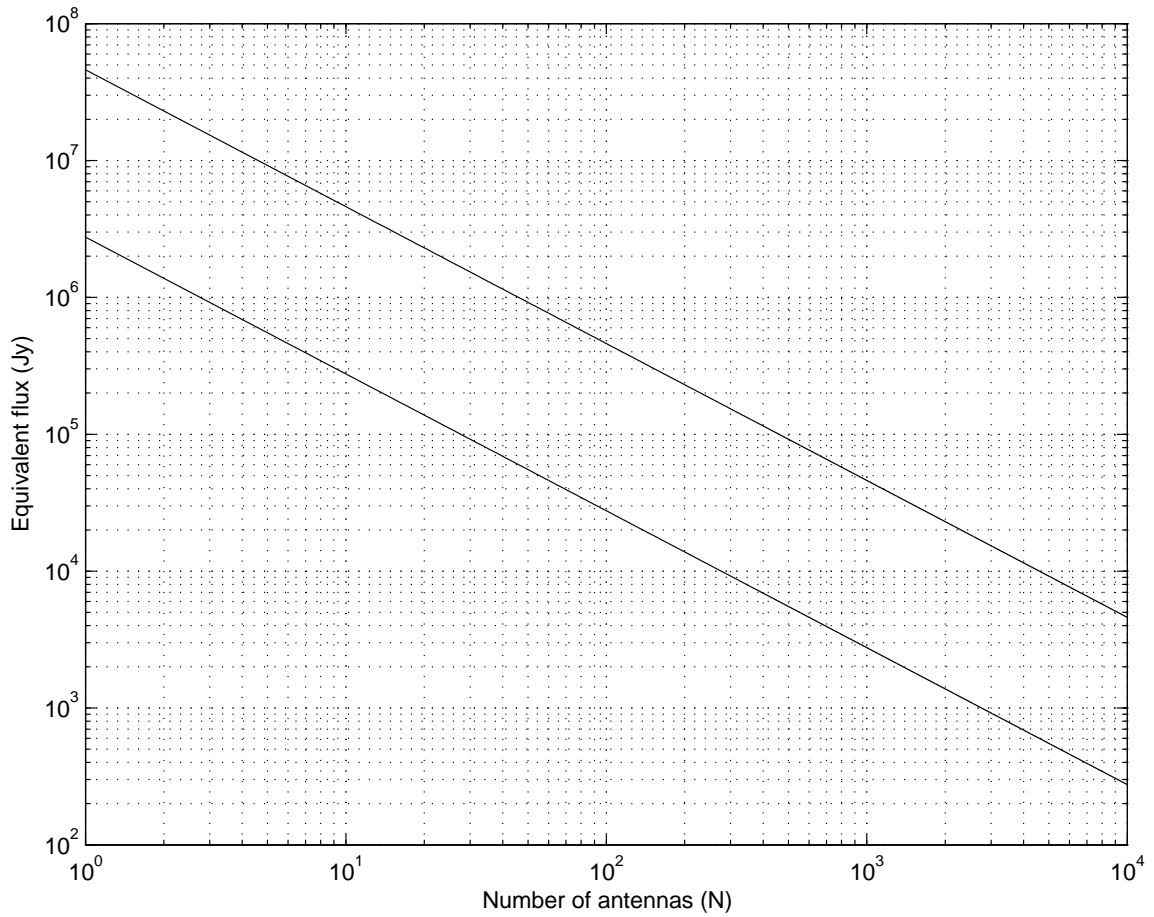


Figure 1: Equivalent flux (Jy) seen by a zenith-pointing beam generated by an Argus with the indicated number of elements (N), due to a background at 100K (top) and 6K (bottom).

Common Name	B	τ for SNR=10	SNR for indicated τ
Iridium	34 kHz*	2.0 μ s	29 dB in 10 ms
GPS C/A (all)	34 kHz*	5.1 ms	21 dB in 1 s
H-I (Global)	34 kHz*	20.5 ms	18 dB in 1 s

Figure 2: Some detectable narrowband sources for an $N = 1$ Argus assuming $\theta = 0$. $*B = 34$ kHz is used here because ANP bandwidth can be at least this large, and because all of the above sources are have bandwidth greater than this. For this reason, two measurements at different tuning frequencies are required for a detection. Night observation is assumed. During the day, noise from the quiet Sun is about 20 dB weaker than the Global H-I line. For the rare occasions that “disturbed sun” conditions apply, only Iridium is detectable: the SNR is bounded in this case to about 16 dB.

3.1 Single-Element (N=1) Argus

Although a single-element Argus may not seem worthwhile to consider, it is in fact useful as a diagnostic configuration and also because $T_g + T_a/N$ has already been experimentally (an approximately) upper-bounded for this case, as noted above, at ~ 100 K. One finds:

$$\Delta S_{N=1} \approx \frac{124 \text{ MJy}}{\cos \theta_m \sqrt{B\tau}}, \quad (13)$$

In an $N = 1$ system, detections are possible only by sensing peaks in the frequency spectrum; therefore only narrowband sources such as spectral lines and SETI signals can possibly be detected. In no case can detected transients be localized, nor can the sky be imaged. On the bright side, only the infrequently disturbed Sun (see source list in the Appendix) – not the quiet (normal) Sun – is strong enough to degrade detection performance across the full tuning range. All other sources of broadband noise are at least an order of magnitude below 124 MJy for $N = 1$ (see Figure 1). Figure 2 identifies some detectable signals.

3.2 N=8 Argus

Detection Sensitivity: An $N = 8$ Argus system has an effective aperture of about $0.05 \cos \theta \text{ m}^2$. The T_a/N term in Equation 9 is not very important since the worst case value of $T_a \sim 100$ K gives $T_a/N \sim 12.5$ K compared to $T_r \sim 170$ K, and even that assumes that a beam is filled with background at that temperature, and neglects the contribution from the ground. Assuming $T_g = 100$ K (very conservative!) and neglecting the T_a/N term, $T_r + T_g + T_a/N \approx 270$ K; in other words, about the same as for the $N = 1$ case. Thus, the sensitivity improves in proportion to the increased aperture, yielding the conservative estimate:

$$\Delta S_{N=8} \approx \frac{15 \text{ MJy}}{\cos \theta_m \sqrt{B\tau}}, \quad (14)$$

Again, the (rarely) disturbed Sun is the only continuum source that can possibly degrade this detection performance.

Imaging and localization with $N = 8$ is very challenging due to the severe limits associated with the array geometry. The antenna units are about 35 cm across, so the closest possible element spacing is ~ 1.7 wavelengths at 1420 MHz, which is 3.4 times the Nyquist criterion for alias-free sampling. Even this is not really practical, since the antenna units are known to interact in a complex way for spacings less than about 3 wavelengths, which is 63 cm at 1420 MHz, or 6 times Nyquist. The recommended geometry for $N = 8$, satisfying the 3-wavelength constraint, is shown in Figure 3.

The sky noise equivalent flux for $N = 8$ varies from ~ 345 kJy at 6K to ~ 5.75 MJy at 100K. Thus, we should have no problem imaging bursts from Iridium and other communications satellites, as long as only one satellite bursts at a given frequency at a time. The disturbed Sun (but not

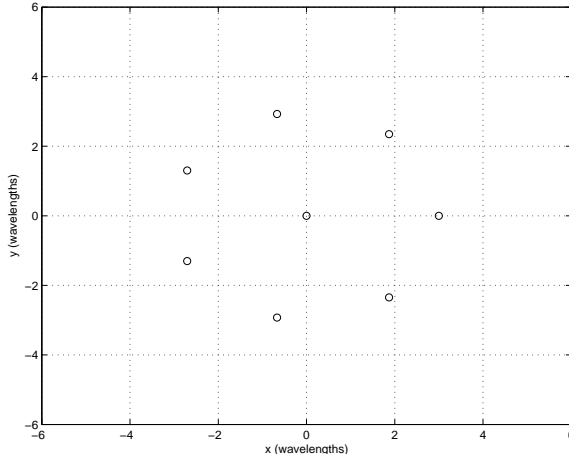


Figure 3: Recommended N=8 array geometry.

the quiet Sun – see below) at 1420 MHz should also be easy to image. Figure 4 shows the all-sky image that would be obtained for one of these sources located at $\theta = 45^\circ$ using this array. Conceptually, this image shows the power measured by a “CBF” beam swept over the entire sky. The conventional beamformer (CBF) maximizes gain in the pointing direction subject to no other constraints (e.g., required nulls). The actual method to make this image would use cross-correlations between elements to avoid beam scanning, but is otherwise equivalent. Also, the $\cos \theta$ effect has been ignored. Figure 4 shows considerable aliasing; however note that the symmetry of the array makes it possible to identify the true source.

It should be noted that C/A transmissions from GPS satellites are well within the detection limits of $N = 8$; however, all GPS satellites transmit all the time, so the severe aliasing exhibited by the array of Figure 3 will make the image hard to understand. An example is shown in Figure 5.

At 1420 MHz, the Sun (quiet or disturbed) is always the strongest discrete continuum radio source in the sky, being at least 20 dB greater than the next strongest discrete continuum source, Cas A. However, the quiet Sun will be just barely detectable (image $\text{SNR} \sim 1$) on a 6K background with $N = 1$ and $B\tau = 1$. However, with just about a second of integration (specifically, $\tau \sim 0.3$ s at $B = 34$ kHz), the quiet Sun could be unambiguously imaged at 1420 MHz on a 100K background.

Imaging Cas A is impractical with $N = 8$ – even at night with large $B\tau$ – because several other sources which are not much weaker (e.g., Sag A, Cyg A) are normally present in the sky at the same time, leading to severe aliasing. Thus, imaging any astrophysical continuum source weaker than the Sun is not really practical for $N = 8$.

3.3 N=16 Argus

Detection Sensitivity: An $N = 16$ Argus system has an effective aperture of about $0.1 \cos \theta \text{ m}^2$. Since the T_a/N term in Equation 9 is not very important, the detection sensitivity is about half that of the $N = 8$ system:

$$\Delta S_{N=16} \approx \frac{8 \text{ MJy}}{\cos \theta_m \sqrt{B\tau}}, \quad (15)$$

Imaging and localization: Although the improvement from $N = 8$ to $N = 16$ doesn’t do much for sensitivity, there is a significant improvement in imaging performance. The recommended geometry for $N = 16$ is shown in Figure 6. For a single source at $\text{SNR} = \infty$, aliasing is negligible and the “image dynamic range” is about 3 dB. Figure 7 is for the same stimulus as Figure 5: 4 equal-strength sources. Note that the image is now understandable. Thus, it should be possible to image GPS with $N = 16$.

To demonstrate the impact of dynamic range, Figure 8 shows the same result as Figure 7, except the source fluxes are varied over about 7 dB.

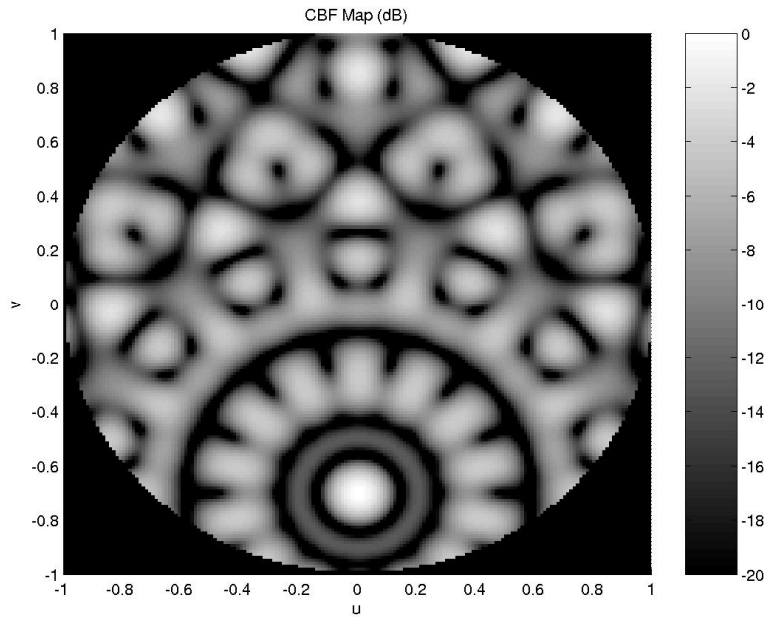


Figure 4: Image of a single source at $\theta = 45^\circ$ using the array shown in Figure 3. $\text{SNR}=\infty$. In this and subsequent images, the zenith is at $u = v = 0$ and the horizon is the circle defined by $u^2 + v^2 = 1$.

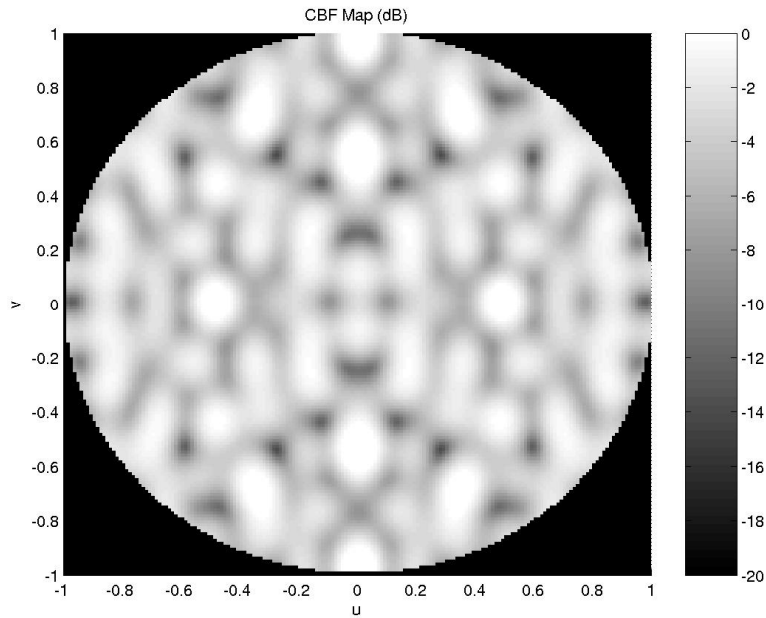


Figure 5: Image of 4 equal-strength sources at $\theta = 45^\circ$ and equally spaced in ϕ , using the $N = 8$ array shown in Figure 3. $\text{SNR}=\infty$.

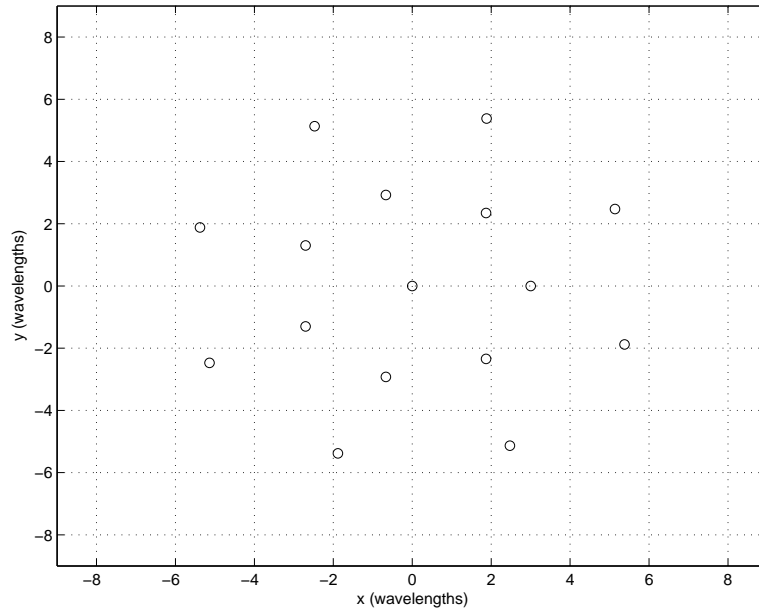


Figure 6: Recommended $N=16$ array geometry.

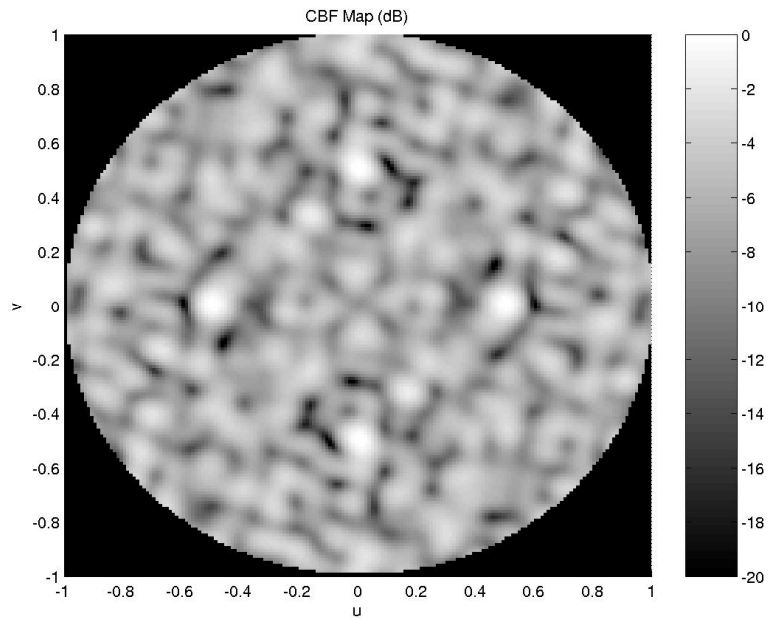


Figure 7: $N = 16$: Image of 4 equal-strength sources at $\theta = 45^\circ$ and equally spaced in ϕ . Image $\text{SNR} = \infty$, image dynamic range ~ 3 dB.

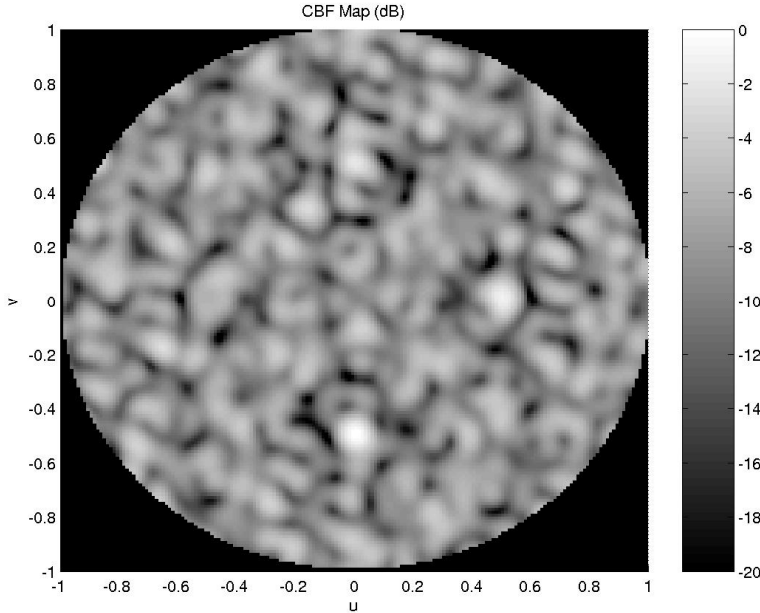


Figure 8: $N = 16$: Simulated sky, with four sources at $\theta = 45^\circ$, equally spaced in ϕ , with relative fluxes of (starting from the 6 o'clock position and moving counter-clockwise) 0 dB, -1.3 dB, -2.2 dB, -7.0 dB. Image SNR = ∞ , image dynamic range ~ 3 dB.

With $N = 8$, the difficulty in imaging astrophysical sources other than the Sun was aliasing, since Cas A, Sag A, and Cyg A are all within 3 dB in flux. This is no longer a problem with $N = 16$, since the imaging dynamic range improves to about 3 dB. Unfortunately, the sky noise equivalent flux for $N = 16$ varies from ~ 173 kJy at 6K to ~ 2.9 MJy at 100K – between 2 and 3 orders of magnitude greater than Cas A. Improving the sensitivity by 3 to 4 orders of magnitude (just to be sure) from an instantaneous SNR of -30 dB requires $B\tau \sim 10^6$ to 10^8 ; or $\tau \sim 30$ s to 49 m for $B = 34$ kHz. This amount of integration time should be possible without much difficulty, although it will be necessary to take sidereal motion into account (the $N = 16$ beam is only about 5° wide). Thus, imaging Cas A, Sag A, and Cyg A should be possible with $N = 16$, provided it is done at night with plenty of integration time.

3.4 $N = 64$ Argus

Detection Sensitivity. An $N = 64$ Argus system has an effective aperture of about $0.38 \cos \theta$ m² in the zenith direction. One finds:

$$\Delta S_{N=64} \approx \frac{2 \text{ MJy}}{\cos \theta_m \sqrt{B\tau}}, \quad (16)$$

Imaging and Localization. Somewhere between $N = 16$ and $N = 64$ elements, pseudorandom arrays start to consistently outperform non-random arrays (assuming both violate Nyquist). The array in Figure 9 was designed using an algorithm that randomly places elements subject to the constraint that the interelement spacing must always be at least 3 wavelengths. Repeating the experiments of Figure 7 and 8 using this array, we obtain Figures 10 and 11 respectively. Note the dramatic improvement in dynamic range, to about 8 dB.

Unfortunately, the sky noise equivalent flux for $N = 64$ varies from ~ 43 kJy at 6K to ~ 725 kJy at 100K – between 1 and 3 orders of magnitude greater than Cas A. We should be able to achieve the same image sensitivity as an $N = 16$ array in one-half the time; $\tau \sim 15$ s to 24 m for $B = 34$ kHz. However, even with 8 dB dynamic range it will be difficult to prevent the sun from dominating the image during the day.

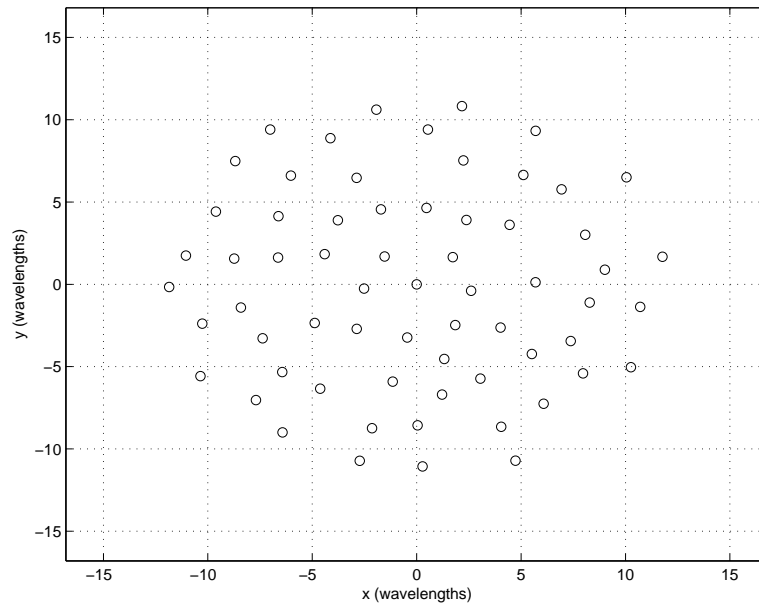


Figure 9: A pseudorandom $N=64$ array geometry generated for this study.

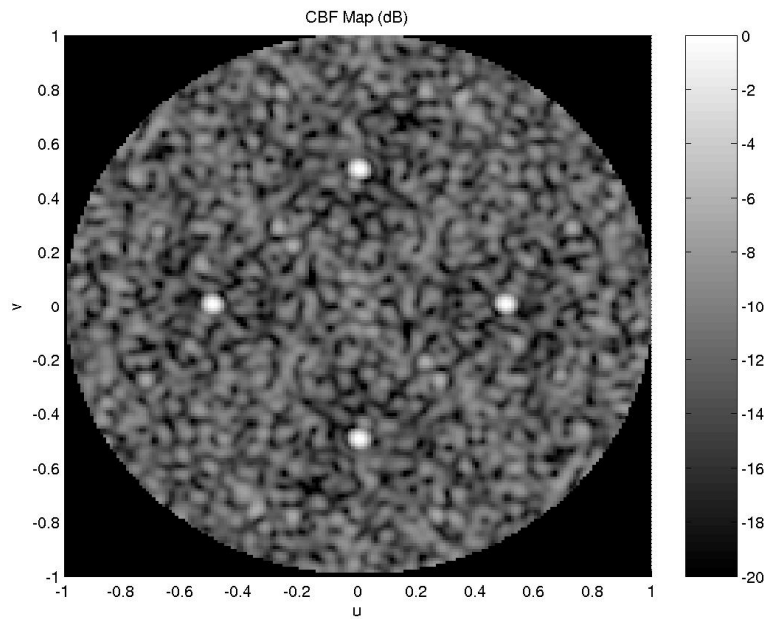


Figure 10: $N = 64$: Image of 4 equal-strength sources at $\theta = 45^\circ$ and equally spaced in ϕ . Image $\text{SNR} = \infty$, image dynamic range ~ 8 dB.

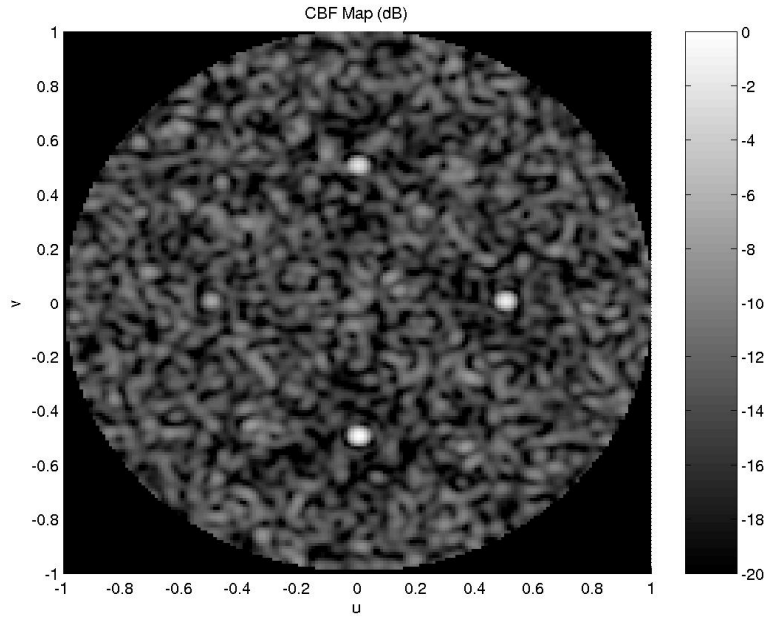


Figure 11: $N = 64$: Dynamic range test, with four sources at $\theta = 45^\circ$, equally spaced in ϕ , with relative fluxes of (starting from the 6 o'clock position and moving counter-clockwise) 0 dB, -1.3 dB, -2.2 dB, -7.0 dB. Image SNR = ∞ , image dynamic range ~ 8 dB.

Acknowledgments

Thanks to R. Dixon and J. Ehman for their helpful comments on this report.

A Source List

Common Name	$S_{1.4 \text{ GHz}}$ Jy	S Jy	Freq. MHz	Description	Remarks	Reference	
Iridium		$\sim 5 \times 10^9$	~ 1624	Single sat	NB burst	[8]	
Unident. sat.		$\sim 2 \times 10^8$	~ 1553	Single sat	NB burst	[8]	
Disturbed Sun ¹		$\sim 1 \times 10^8$	L-Band			[5], p. 8-12	
Unident. sat.		$\sim 1 \times 10^8$	~ 1557	Single sat	NB burst	[8]	
GPS C/A (all)	$\sim 5 \times 10^7$	$\sim 1 \times 10^8$	1575.42	All visible sats	2 MHz BW	[8]	
H-I (Global)				Hydrogen Line	100 kHz BW	[9]	
GPS C/A (one)		$\sim 2 \times 10^7$	1575.42	Single sat	2 MHz BW	[8]	
GPS P (all)		$\sim 1 \times 10^7$	1575.42	All visible sats	20 MHz BW	[8]	
GPS P (one)		$\sim 2 \times 10^6$	1575.42	Single sat	20 MHz BW	[8]	
Quiet Sun			$\sim 3 \times 10^5$	L-Band			[6], p. 110
Cas A ²		2477	3300	1000	SNR	3C461	[7], p. 147, 149
Cyg A ²		1495	2340	1000	Galaxy	3C405	[7], p. 146, 149
Sag A			2000	1000	Galactic Center		[7], p. 146
Moon			~ 1000	1000			[5], p. 8-12
Omega Nebula	1000			H-II region	M17	[5], p. 8-87	
		800	1000			[7], p. 146	
Tau A ²	875	955	1000	SNR, Crab Neb.	M1	[7], p. 145, 148	
Cyg X		400	1000	H-II region		[7], p. 147	
3C400	576	400	1000			[7], p. 146, 149	
N. Am. Nebula	550			H-II region	3C400	[5], p. 8-87	
Ori A	520	340	1000	H-II region	M42, 3C145	[7], p. 145, 148	
Rosette Neb.	260			H-II region		[5], p. 8-87	
		250	1000			[7], p. 145	
Lagoon Neb.	260			H-II region	M8	[5], p. 8-87	
		150	1000			[7], p. 146	
3C274	214	*	*	Cal data avail.		[7], p. 151-2	
Vir A ²	198	263	1000	Galaxy	M87, 3C274	[7], p. 145, 148	
3C392	171	210	1000	SNR	3C392	[7], p. 149	
3C157		180	1000		3C157	[7], p. 145	
Pup A		150	1000			[7], p. 145	
For A	115			Galaxy		[7], p. 148	
Andromeda		100	L-Band	Galaxy	M31	[6], p. 110	
3C273		80	L-Band	SNR	3C273	[6], p. 110	
3C295		30	L-Band		3C295	[5], p. 8-12	
	*	*	*	Cal data avail.		[7], p. 151	
Jupiter		8	L-Band	synchrotron emm.		[5], p. 8-70	

¹ This condition rarely occurs.

² See also http://www.astron.nl/reduce/dwingeloo/text_for_titus/texinfo/html/dwingeloo.6.html.

References

- [1] R.S. Dixon, "Argus: A Next-Generation Omnidirectional Radio Telescope," *Proc. High-Sensitivity Radio Astronomy*, University of Manchester, England, January 1996. Reprinted in N. Jackson and R.J. Davies, *High-Sensitivity Radio Astronomy*, Cambridge University Press, 1997, pp. 260-8.
- [2] J. Tarter, J. Dreher, S.W. Ellingson, and W.J. Welch, "Recent Progress and Activities in the Search for Extraterrestrial Intelligence (SETI)," Chapter 36 of *Review of Radio Science, 1999-2002*, W. Ross Stone (Ed.), IEEE Press/John Wiley, 2002.
- [3] ESL Argus Document Server, <http://esl.eng.ohio-state.edu/~swe/argus/docserv.html>.
- [4] G. Hampson and S. Ellingson, "A New Argus Direct Conversion Receiver and Digital Array Receiver/Processor," Design Report, September 27, 2002. Available at <http://esl.eng.ohio-state.edu/~swe/argus/docserv.html>.
- [5] J.D. Kraus, *Radio Astronomy*, 2nd Ed., Cygnus-Quasar, 1986.
- [6] B.F. Burke and F. Graham-Smith, *An Introduction to Radio Astronomy*, Cambridge University Press, 1997.
- [7] M.V. Zombeck, *Handbook of Space Astronomy and Astrophysics*, 2nd Ed., Cambridge University Press, 1990.
- [8] S.W. Ellingson, "RFI at SCF as Seen by Argus," Oct 19, 2002. Available at <http://esl.eng.ohio-state.edu/~swe/argus/docserv.html>.
- [9] S.W. Ellingson, "A High-Resolution Survey of RFI at 1200-1470 MHz as Seen by Argus," Oct 29, 2002. Available at <http://esl.eng.ohio-state.edu/~swe/argus/docserv.html>.